

# Journal of Materials Chemistry C

Accepted Manuscript



This is an *Accepted Manuscript*, which has been through the Royal Society of Chemistry peer review process and has been accepted for publication.

*Accepted Manuscripts* are published online shortly after acceptance, before technical editing, formatting and proof reading. Using this free service, authors can make their results available to the community, in citable form, before we publish the edited article. We will replace this *Accepted Manuscript* with the edited and formatted *Advance Article* as soon as it is available.

You can find more information about *Accepted Manuscripts* in the [Information for Authors](#).

Please note that technical editing may introduce minor changes to the text and/or graphics, which may alter content. The journal's standard [Terms & Conditions](#) and the [Ethical guidelines](#) still apply. In no event shall the Royal Society of Chemistry be held responsible for any errors or omissions in this *Accepted Manuscript* or any consequences arising from the use of any information it contains.

# Room temperature ferromagnetism in $(\text{Ga}_{1-x}\text{Mn}_x)_2\text{O}_3$ epitaxial thin films

Daoyou Guo,<sup>ab</sup> Zhenping Wu,<sup>ab</sup> Yuehua An,<sup>ab</sup> Xiaojiang Li,<sup>c</sup> Xuncai Guo,<sup>ab</sup> Xulong Chu,<sup>ab</sup> Changlong Sun,<sup>ab</sup>

Ming Lei,<sup>ab</sup> Linghong Li,<sup>f</sup> Lixin Cao,<sup>d</sup> Peigang Li<sup>\*ac</sup> and Weihua Tang<sup>\*ab</sup>

<sup>a</sup> School of Science, Beijing University of Posts and Telecommunications, Beijing 100876, China.

<sup>b</sup> State Key Laboratory of Information Photonics and Optical Communications, Beijing University of Posts and Telecommunications, Beijing 100876, China. E-mail: [whtang@bupt.edu.cn](mailto:whtang@bupt.edu.cn) (Weihua Tang)

<sup>c</sup> Center for Optoelectronics Materials and Devices, Department of Physics, Zhejiang Sci-Tech University, Hangzhou 310018, Zhejiang, China. E-mail: [pgli@zstu.edu.cn](mailto:pgli@zstu.edu.cn) (Peigang Li)

<sup>d</sup> Beijing National Laboratory for Condensed Matter Physics, Institute of Physics, Chinese Academy of Science, Beijing 100190, China.

<sup>e</sup> State key Laboratory of Functional Materials for Informatics, Shanghai Institute of Microsystem and Information Technology, Chinese Academy of Sciences, Shanghai 200050, China.

<sup>f</sup> Department of Physics, The State University of New York at Potsdam, Potsdam, New York 13676-2294, USA.

Mn-doped monoclinic  $\beta$ -(Ga<sub>1-x</sub>Mn<sub>x</sub>)<sub>2</sub>O<sub>3</sub> thin films were epitaxially grown on  $\alpha$ -Al<sub>2</sub>O<sub>3</sub> (0001) substrates by alternately depositing Ga<sub>2</sub>O<sub>3</sub> and Mn layers using the laser molecular beam epitaxy technique. The crystal lattice expands and the energy band gap shrinks with the increase of Mn content for Mn ion incorporated into Ga site. Ferromagnetism appears even above room temperature when  $x \geq 0.11$  and can be remarkably enhanced with the continuous increase of Mn indicated by the increased magnetization and coercivity. The study presents a promising candidate for use in spintronics devices that are capable of working at room temperature.

## Introduction

Magnetic semiconductors have attracted considerable attentions for their potential applications in spintronics devices,<sup>1-5</sup> such as fast nonvolatile semiconductor memories and integrated magnetic/electronic/photonic devices. According to the theoretical prediction by Dietl,<sup>6</sup> high Curie temperature ( $T_c$ ) even exceeding room temperature could be achieved in some wide band gap semiconductors when they are doped with transition metals, especially Mn. The thus-far doping work has been carried out mainly in some conventional II-VI and III-V compounds,<sup>7-12</sup> such as (Ga,Mn)As, (In,Mn)As, (Ga,Mn)N and (Zn,Mn)O, etc., while mechanism for the appearance of ferromagnetism remains rather elusive. The discovery of more ferromagnetic semiconductors is always desired not only because they can provide complementary knowledge helpful for clarifying the fundamental issue but also due to their potential practical applications. Gallium oxide ( $\text{Ga}_2\text{O}_3$ ), a wide direct band gap semiconductor with a gap size of  $\sim 4.9$  eV,<sup>13-15</sup> is a good place for such exploration. High photon energy and high transparency in the visible and ultraviolet region ( $> 280$  nm) enable the easy manipulation of the spins by photons, and thus make  $\text{Ga}_2\text{O}_3$  attractive for use in spintronics devices.

$\text{Ga}_2\text{O}_3$  can crystalize in five different phases (known as  $\alpha$ ,  $\beta$ ,  $\gamma$ ,  $\delta$ , and  $\epsilon$ -phases).<sup>16</sup> Among these, the monoclinic  $\beta$ - $\text{Ga}_2\text{O}_3$  (space group:  $C2/m$ ) with the lattice parameters of  $a = 12.23$  Å,  $b = 3.04$  Å,  $c = 5.80$  Å, and  $\beta = 103.7^\circ$  has been recognized as the most stable phase suitable for various characterizations and more intensively studied.<sup>16-18</sup> Ferromagnetism was observed in Mn-doped  $\gamma$ - $\text{Ga}_2\text{O}_3$  at room temperature as well as in highly crystalline corundum-structured  $\alpha$ - $(\text{Ga}_{1-x}\text{Fe}_x)_2\text{O}_3$  ( $x=0.58$ ) thin film.<sup>19-21</sup> However,

magnetic properties of Mn-doped  $\beta$ -Ga<sub>2</sub>O<sub>3</sub> have not been studied yet. In this work, we report on the observation of ferromagnetism even above room temperature in epitaxially grown Mn-doped  $\beta$ -Ga<sub>2</sub>O<sub>3</sub> thin films with high Mn concentrations.

## Experimental

The film growth of Mn-doped  $\beta$ -Ga<sub>2</sub>O<sub>3</sub> was performed by using the laser molecular beam epitaxy technique with a pulse energy density of  $\sim 5$  J/cm<sup>2</sup> on  $\alpha$ -Al<sub>2</sub>O<sub>3</sub> (0001) substrates at 900 °C. The Ga<sub>2</sub>O<sub>3</sub> and Mn layers were alternately deposited and both depositions were repeated for 20 times. The Mn concentrations were controlled by solely changing the laser pulse numbers during each run of depositing the Mn layers (defined as N, N=10, 20, 30, 40, 50) while those for depositing Ga<sub>2</sub>O<sub>3</sub> layers in each run were fixed at 100. The alternating deposition enabled the realization of (Ga<sub>1-x</sub>Mn<sub>x</sub>)<sub>2</sub>O<sub>3</sub> thin films with different compositions due to inter diffusion between Mn and Ga<sub>2</sub>O<sub>3</sub> layers at high temperature. The Mn concentrations in (Ga<sub>1-x</sub>Mn<sub>x</sub>)<sub>2</sub>O<sub>3</sub> films were determined as 6.06 at.%, 10.97 at.%, 17.64 at.%, 31.17 at.%, and 53.10 at.% respectively by the X-ray energy dispersive spectroscopy (EDS). The orientation and crystallinity of the as-grown films were investigated by X-ray diffraction (XRD) at  $\theta$ -2 $\theta$  scan and *in-situ* reflection high-energy electron diffraction (RHEED). The valences of Mn ions and elements distribution were analyzed by X-ray photoelectron spectroscopy (XPS) and secondary ion mass spectrometry (SIMS). Magnetic properties of the films were measured in a commercial superconducting quantum interference device (SQUID), Quantum design.

## Results and discussion

The crystal structures of the as-grown films were characterized from  $\theta$ - $2\theta$  scans of XRD, the results are shown in Fig. 1(a). Except diffraction peaks of the  $\text{Al}_2\text{O}_3$  substrate, only diffraction peaks located at around  $19^\circ$ ,  $38^\circ$ , and  $59^\circ$  were observed, all of them belongs to  $(\text{Ga}_{1-x}\text{Mn}_x)_2\text{O}_3$ . No peaks from Mn metal clusters, Mn oxide,  $\text{Mn}_x\text{Ga}_y$  or  $\text{MnGa}_2\text{O}_4$  phases were exist. As seen from the enlarged view of  $\theta$ - $2\theta$  XRD patterns around  $38^\circ$  (Fig. 1(b)), the peaks are located at  $38.34^\circ$ ,  $38.12^\circ$ ,  $37.94^\circ$ ,  $37.77^\circ$ ,  $37.60^\circ$ , and  $37.15^\circ$  for  $x=0, 0.06, 0.11, 0.18, 0.31$ , and  $0.53$ , respectively, indicating that the peak gradually shifts to smaller  $2\theta$  with the increase of  $x$ . Meanwhile, no abrupt shift or half height width changing of diffraction peak were observed with the increase of  $x$  (the relative large shift for  $x=0.53$  may be attributed to the relative much increase of Mn content from 0.31 to 0.53). Thus, the possibility of phase transformation would be excluded. According to relevant references, the  $(\bar{2}01)$  diffraction peak of  $\beta\text{-Ga}_2\text{O}_3$  (PDF#43-1012) and the  $(222)$  diffraction peak of  $\gamma\text{-Ga}_2\text{O}_3$  (References 19 and 20) should be located at  $38.40^\circ$  and  $37.28^\circ$ , respectively. For  $x=0.06$ , if  $\gamma$ -phase appears, the diffraction peak around  $38^\circ$  should present an abrupt shift to near, even lower than  $37.28^\circ$  due to Mn doping. Actually, the peak locates at  $38.12^\circ$  which is closer to the  $38.40^\circ$  of  $\beta$ -phase. Thus, we believe that  $\beta\text{-Ga}_2\text{O}_3$  is obtained by Mn-doping. The diffraction peaks located at around  $19^\circ$ ,  $38^\circ$ , and  $59^\circ$  are correspond to  $(\bar{2}01)$  and higher order peaks of monoclinic  $\beta$ -phase  $\text{Ga}_2\text{O}_3$  respectively, indicating a preferred  $(\bar{2}01)$  plane orientation of the thin films. The  $x$  dependence of  $(\bar{2}01)$  plane distance is depicted in Fig. 1(c), showing that the  $d$  spacing increases almost linearly

with the increase of  $x$ . With the increase of  $x$ , the peak shift of  $(\bar{2}01)$  plane to smaller  $2\theta$  indicates a gradual increase of the lattice constants because the radii of Mn ions are larger than that of Ga ion (Mn<sup>2+</sup>, Mn<sup>3+</sup> and Ga<sup>3+</sup> ionic radii are 0.83, 0.64 and 0.62 Å, respectively).<sup>22,23</sup> These facts, along with the EDS results, demonstrate the successful incorporation of Mn ions into the lattice of Ga<sub>2</sub>O<sub>3</sub>. The clear and streaky RHEED patterns shown by Fig. 1(d) suggest that the (Ga<sub>1-x</sub>Mn<sub>x</sub>)<sub>2</sub>O<sub>3</sub> films are of single phase with very smooth surfaces.

Hayashi *et al.* reported that Mn-doped Ga<sub>2</sub>O<sub>3</sub> (7 cation % of Mn) thin film grown at 500° exhibits spinel structure of  $\gamma$ -phase.<sup>19</sup> According to the temperature dependent phases transformation by Roy,<sup>16</sup>  $\gamma$ -phase is metastable and would transfer to the stable monoclinic  $\beta$ -phase above 650°C. It is reasonable for Mn-doped Ga<sub>2</sub>O<sub>3</sub> thin film exhibiting  $\gamma$ -phase when the films deposited at 500°C. When the deposition temperature is above 600°C,  $\beta$ -Ga<sub>2</sub>O<sub>3</sub> will appear in Mn-doped Ga<sub>2</sub>O<sub>3</sub> films,<sup>24</sup> indicating that the transformation of  $\gamma$ -phase to  $\beta$ -phase has began at 600°C. Herein, the (Ga<sub>1-x</sub>Mn<sub>x</sub>)<sub>2</sub>O<sub>3</sub> thin films were growth with a substrate temperature of 900°C, all the metastable phases would be transfer to  $\beta$  phases. We have characterized the (Ga<sub>1-x</sub>Mn<sub>x</sub>)<sub>2</sub>O<sub>3</sub> thin film with  $x=0.06$  using selected-area electron diffraction patterns in an orientation parallel to the  $(10\bar{1}0)$  of Al<sub>2</sub>O<sub>3</sub> substrate, and the results confirmed the obtained film was  $\beta$ -Ga<sub>2</sub>O<sub>3</sub>.<sup>20</sup> More sophisticated research is under way.

Compositions as a function of film thickness were also characterized by using the SIMS depth profiling. The results for the representative (Ga<sub>0.47</sub>Mn<sub>0.53</sub>)<sub>2</sub>O<sub>3</sub> film were summarized in Fig. 2 by showing intensities of the Mn and Ga ion currents as a function

of sputter depth of the film. Intensities of both Mn and Ga ion currents remain almost constant indicating that Mn is actually uniformly distributed in the film without any detectable enrichment or segregation. Meanwhile, the streak lines of RHEED patterns always keep sharp during the growth processes, indicating that Mn ions are uniformly distributed in-plane. These results thus evidently excludes the possibility of formation of Mn-rich layers in  $(\text{Ga}_{1-x}\text{Mn}_x)_2\text{O}_3$  thin films.

The chemical compositions and chemical states of Mn ions in the films were characterized by using XPS, presented in Fig. 3. The elements present in the  $(\text{Ga}_{0.47}\text{Mn}_{0.53})_2\text{O}_3$  film are Mn, Ga, O, and C (not shown). The charge-shift spectrum was calibrated using the fortuitous C 1s peak at 284.8 eV. The spectrum of Mn 2p shows a spin-orbit doublet ( $j = 3/2, 1/2$ ). The Mn  $2p_{3/2}$  main peak has a satellite structure on the higher binding-energy side separated by  $\sim 6$  eV, which indicates a strong Coulomb interaction between the Mn 3d electrons and hybridization between the Mn 3d and other valence orbitals.<sup>25</sup> No Mn  $2p_{3/2}$  peaks for metallic Mn (located at 639 eV) are visible in Fig. 3, indicating no Mn metallic clusters present in the films.<sup>26</sup> It is also noted that Mn  $2p_{3/2}$  main peak contains two peaks corresponding to 640.59 and 641.74 eV, respectively, implying the presence of two possible valence states ( $\text{Mn}^{2+}/\text{Mn}^{3+}$ ) with a ratio of about 19:81. The neutral configuration of Mn in  $\text{Ga}_2\text{O}_3$  should be  $\text{Mn}^{3+}$  when viewed as replacing  $\text{Ga}^{3+}$  in the lattice. However, there are many oxygen vacancies as donor-type defects in  $\beta\text{-Ga}_2\text{O}_3$  thin films, which would lead to the valence of Mn change from +3 to +2.<sup>14</sup> In addition, seen from the XPS spectrum of Ga 3d core-level in the inset of Fig. 3, there is only one peak at 20.4 eV, which comes from the Ga ions in the  $(\text{Ga}_{1-x}\text{Mn}_x)_2\text{O}_3$



films.<sup>27</sup> And another peak at  $\sim 18.4$  eV for decomposed Ga atoms cannot be found,<sup>27</sup> suggesting that the metallic Ga or  $\text{Mn}_x\text{Ga}_y$  are not present in our samples.

The band gap of  $(\text{Ga}_{1-x}\text{Mn}_x)_2\text{O}_3$  thin films can be modified by changing the Mn content, indicated by the ultraviolet-visible (UV-Vis) absorbance measurements. Shown by the absorbance spectra of  $(\text{Ga}_{1-x}\text{Mn}_x)_2\text{O}_3$  ( $x=0, 0.11, 0.31$ ) thin films in Fig. 4, the spectrum of the host exhibits a sharp intrinsic absorption edge at  $\sim 250$  nm,<sup>28</sup> whilst those of Mn-doped samples display clear red-shift. The gap sizes can be derived by fitting the linear region of the  $(\alpha h\nu)^2$  versus  $h\nu$  plot, shown by the inset to Fig. 4. The gap size decreases from 4.92 eV for  $x = 0$  to 4.87 eV and 4.72 eV for  $x = 0.11$  and  $x=0.31$ , respectively.

Figure 5 shows the magnetization versus magnetic field ( $M$ - $H$ ) curves of  $(\text{Ga}_{1-x}\text{Mn}_x)_2\text{O}_3$  films at room temperature measured with the applied magnetic field parallel to the films. The diamagnetic contribution from the sapphire substrate was subtracted from the data. The  $(\text{Ga}_{0.94}\text{Mn}_{0.06})_2\text{O}_3$  film displays typical paramagnetic behavior while  $(\text{Ga}_{1-x}\text{Mn}_x)_2\text{O}_3$  thin films with  $x \geq 0.11$  show hysteresis loops indicative of ferromagnetism. However, for  $\gamma$ -phase Mn-doped  $\text{Ga}_2\text{O}_3$ , the film with Mn concentration even of 7% has shown room temperature ferromagnetism with a magnetization of  $2.8 \text{ emu/cm}^3$  at 2 kOe,<sup>19</sup> which may be attributed to different phase type of  $(\text{Ga}_{1-x}\text{Mn}_x)_2\text{O}_3$  thin films. Magnetic parameters for  $(\text{Ga}_{1-x}\text{Mn}_x)_2\text{O}_3$  films with respect to  $x$  are listed in Table 1. The saturation magnetizations ( $M_s$ ) increase monotonically from  $5.5 \text{ emu/cm}^3$  to the maximum value of  $33.1 \text{ emu/cm}^3$  at 2 kOe with the increase of  $x$  and the coercivity and magnetic remanence ( $M_r$ ) increase as well,

revealing apparent enhancement of ferromagnetism with the increase of Mn content. For  $(\text{Ga}_{0.47}\text{Mn}_{0.53})_2\text{O}_3$  film, the coercivity and  $M_r$  reach  $\sim 109$  Oe and  $7.6$  emu/cm<sup>3</sup>, respectively. The temperature dependent magnetization ( $M$ - $T$ ) of  $(\text{Ga}_{0.47}\text{Mn}_{0.53})_2\text{O}_3$  film was measured at 2 kOe using field-cooling mode. Seen from the  $M$ - $T$  curve shown in the inset of Fig. 5,  $M$  is seen to be fairly constant in the measurement temperature range of 15 ~ 400 K.

The above XRD, SIMS, XPS, UV-Vis absorption, and magnetic properties characterizations on  $(\text{Ga}_{1-x}\text{Mn}_x)_2\text{O}_3$  films are sufficient to confirm the successful substitution of Mn for Ga. Meanwhile, according to the XRD and XPS analyses, we did not find any room ferromagnetic second phase, such as  $\text{Mn}_x\text{Ga}_y$  clusters. Nevertheless, for the possible secondary phases of Mn metal and Mn-based oxides, only  $\text{Mn}_3\text{O}_4$  is ferromagnetic with a small  $T_c$  of 43 K while others are all antiferromagnetic.<sup>10,29</sup> It is reasonably to conclude that the room temperature ferromagnetism in the  $(\text{Ga}_{1-x}\text{Mn}_x)_2\text{O}_3$  thin films with high Mn concentrations is intrinsic.

Up to now, there is no a perfect model that can well describe the origin of the room-temperature ferromagnetism of Mn-doped  $\text{Ga}_2\text{O}_3$ . Hayashi *et al.*<sup>19</sup> suggested that the room temperature ferromagnetism of  $\gamma$ - $(\text{Ga}_{1-x}\text{Mn}_x)_2\text{O}_3$  can be explained by a carriers-mediated double exchange model that had been used to explain room temperature ferromagnetism in Mn-doped GaN. Pei *et al.*<sup>30</sup> also used the model to propose the ferromagnetic coupling in their theoretical study on magnetic properties of Mn-doped  $\beta$ - $\text{Ga}_2\text{O}_3$  and pointed out that the ferromagnetic ground state could be established even at a small Mn concentration of 12.5 at.%. For the carrier-mediated

double exchange model, a large quantity of mobile carriers are desired to induce ferromagnetism.<sup>4,31</sup> However, in our system, the charge carriers should be highly localized due to the high intrinsic properties of  $\beta$ -Ga<sub>2</sub>O<sub>3</sub> hosts, as a result, we failed to measure the carrier type and carrier concentration in (Ga<sub>1-x</sub>Mn<sub>x</sub>)<sub>2</sub>O<sub>3</sub> thin films using Hall Effect measurement. So the framework of bound magnetic polaron (BMP) model should be more suitable. In the BMP model, ferromagnetic exchange is mediated through localized donor electrons in the impurity band.<sup>32</sup> The interactions of BMPs in an insulator follow essentially from the Loss and DiVincenzo<sup>33</sup> proposal for spin-based solid-state quantum computing electrons localized in electrostatically defined quantum dots, with coupling between electron spins via the exchange interaction. Base on doping level, the ferromagnetism coupling could be classified to three main processes in BMP model.<sup>34-35</sup> In minor-doped, the remote impurities produce low magnetic moments for weak interaction. In appropriate-doped, a sufficiently large number of bound magnetic polarons long-range ferromagnetic order would be established. While in heavy-doped, the increase of dopant concentration will strengthen dopant-dopant associations and leads to progressive orbital moment quenching, causing the decrease of the ferromagnetism. The BMP model seems to be more suitable for our experiment results, but it does not mean that the BMP is a satisfied model to explain room-temperature ferromagnetism in (Ga<sub>1-x</sub>Mn<sub>x</sub>)<sub>2</sub>O<sub>3</sub>. In order to deeper understand the mechanism, more experimental and theoretical works should be done to improve the current models or propose a better model.

## Conclusions

In conclusion, monoclinic  $(\text{Ga}_{1-x}\text{Mn}_x)_2\text{O}_3$  thin films with a preferable  $(\bar{2}01)$  orientation on  $\alpha\text{-Al}_2\text{O}_3$  (0001) substrates were epitaxially grown by using laser molecular beam epitaxy technique. The systematic characterizations by XRD, SIMS, XPS and UV-Vis absorbance spectrum confirmed the incorporation of Mn into the lattice of  $\beta\text{-Ga}_2\text{O}_3$  and revealed its effects on the crystal and electronic structures. Magnetic properties measurements revealed that the  $(\text{Ga}_{1-x}\text{Mn}_x)_2\text{O}_3$  thin films are ferromagnetic even above room temperature, and the ferromagnetism can be enhanced with increasing the Mn content.

### Acknowledgements

This work was supported by the National Natural Science Foundation of China (No. 61274017, 51172208, 11404029), Fund of State Key Laboratory of Information Photonics and Optical Communications (BUPT), the Beijing University of Posts and Telecommunications (BUPT) Excellent Ph.D. Students Foundation (No. CX201421), China Postdoctoral Science Foundation Funded Project (Grant No. 2014M550661), the Fundamental Research Funds for the Central Universities (Grant No. 2014RC0906), and National Basic Research Program of China (973 Program) (2010CB923202).

**References**

- <sup>1</sup> S. Wolf, D. Awschalom, R. Buhrman, J. Daughton, S. Von Molnar, M. Roukes, A. Y. Chtchelkanova and D. Treger, *Science*, 2001, **294**, 1488.
- <sup>2</sup> L. Chen, L. Guo, Z. Li, H. Zhang, J. Lin, J. Huang, S. Jin and X. Chen, *Sci. Rep.*, 2013, **3**, 2599.
- <sup>3</sup> S. Fusil, V. Garcia, A. Barthélémy and M. Bibes, *Annu. Rev. Mater. Res.*, 2014.
- <sup>4</sup> X. Lia and J. Yang, *J. Mater. Chem. C*, 2014, **2**, 7071.
- <sup>5</sup> Y. Liu, G. Wang, S. Wang, J. Yang, L. Chen, X. Qin, B. Song, B. Wang and X. Chen, *Phys. Rev. Lett.*, 2011, **106**, 087205.
- <sup>6</sup> T Dietl, H Ohno, F Matsukura, J Cibert and D Ferrand, *Science*, 2000, **287**, 1019.
- <sup>7</sup> A. MacDonald, P. Schiffer and N. Samarth, *Nat. Mater.*, 2005, **4**, 195.
- <sup>8</sup> Y. Liu, L. Jiang, G. Wang, S. Zuo, W. Wang and X. Chen, *Appl. Phys. Lett.*, 2012, **100**, 122401.
- <sup>9</sup> N. Theodoropoulou, A. Hebard, M. Overberg, C. Abernathy, S. Pearton, S. Chu and R. Wilson, *Phys. Rev. Lett.*, 2002, **89**, 107203.
- <sup>10</sup> S. Jung, S. J. An, G. C. Yi, C. Jung, S. I. Lee and S. Cho, *Appl. Phys. Lett.*, 2002, **80**, 4561.
- <sup>11</sup> S. Sonoda, I. Tanaka, F. Oba, H. Ikeno, H. Hayashi, T. Yamamoto, Y. Yuba, Y. Akasaka, K. Yoshida, M. Aoki, M. Asari, T. Araki, Y. Nanishi, K. Kindo and H. Hori, *Appl. Phys. Lett.*, 2007, **90**, 012504.
- <sup>12</sup> B. Song, K. Zhu, J. Liu, J. Jian, J. Han, H. Bao, H. Li, Y. Liu, H. Zuo, W. Wang, G. Wang, X. Zhang, S. Meng, W. Wang and X. Chen, *J. Mater. Chem.*, 2010, **20**, 9935.

- <sup>13</sup> W. Feng, X. Wang, J. Zhang, L. Wang, W. Zheng, P. Hu, W. Cao and B. Yang, *J. Mater. Chem. C*, 2014, **2**, 3254.
- <sup>14</sup> D. Y. Guo, Z. P. Wu, Y. H. An, X. C. Guo, X. L. Chu, C. L. Sun, L. H. Li, P. G. Li and W. H. Tang, *Appl. Phys. Lett.*, 2014, **105**, 023507.
- <sup>15</sup> T. Oshima, T. Okuno, N. Arai, N. Suzuki, S. Ohira and S. Fujita, *Appl. Phys. Express*, 2008, **1**, 011202.
- <sup>16</sup> R. Roy, V. Hill and E. Osborn, *J. Am. Chem. Soc.*, 1952, **74**, 719.
- <sup>17</sup> K. Matsuzaki, H. Yanagi, T. Kamiya, H. Hiramatsu, K. Nomura, M. Hirano and H. Hosono, *Appl. Phys. Lett.*, 2006, **88**, 092106.
- <sup>18</sup> K. Matsuzaki, H. Hiramatsu, K. Nomura, H. Yanagi, T. Kamiya, M. Hirano and H. Hosono, *Thin Solid Films*, 2006, **496**, 37.
- <sup>19</sup> H. Hayashi, R. Huang, H. Ikeno, F. Oba, S. Yoshioka, I. Tanaka and S. Sonoda, *Appl. Phys. Lett.*, 2006, **89**, 181903.
- <sup>20</sup> R. Huang, H. Hayashi, F. Oba and I. Tanaka, *J. Appl. Phys.*, 2007, **101**, 063526.
- <sup>21</sup> K. Kaneko, I. Takeya, S. Komori and S. Fujita, *J. Appl. Phys.*, 2013, **113**, 233901.
- <sup>22</sup> Y. An, S. Wang, L. Duan, J. Liu and Z. Wu, *Appl. Phys. Lett.*, 2013, **102**, 212411.
- <sup>23</sup> Y. Kokubun, K. Miura, F. Endo and S. Nakagomi, *Appl. Phys. Lett.*, 2007, **90**, 031912.
- <sup>24</sup> H. Hayashi, R. Huang, F. Oba, T. Hirayama and I. Tanaka, *J. Mater. Res.*, 2011, **26**, 578.
- <sup>25</sup> J. Okabayashi, A. Kimura, O. Rader, T. Mizokawa, A. Fujimori, T. Hayashi, and M. Tanaka, *Phys. Rev. B* 1998, **58**, R4211.

- <sup>26</sup> J. F. Moudler, W. F. Stickle, P. E. Sobol and K. D. Bomben, *Handbook of X-Ray Photoelectron Spectroscopy* (Perkin-Elmer, Eden Prairie, 1992).
- <sup>27</sup> B. Hu, B. Y. Man, C. Yang, M. Liu, C. S. Chen, X. G. Gao, S. C. Xu, C. C. Wang and Z. C Sun, *Appl. Surf. Sci.*, 2011, **258**, 525.
- <sup>28</sup> D. Y. Guo, Z. P. Wu, P. G. Li, Y. H. An, H. Liu, X. C. Guo, H. Yan, G. F. Wang, C. L. Sun, L. H. Li and W. H. Tang, *Opt. Mater. Express*, 2014, **4**, 1067.
- <sup>29</sup> T. Suzuki and T. Katsufuji, *Phys. Rev. B*, 2008, **77**, 220402(R).
- <sup>30</sup> G. Pei, C. Xia, Y. Dong, B. Wu, T. Wang and J. Xu, *Scripta Mater.*, 2008, **58**, 943.
- <sup>31</sup> N. Khare, M. J. Kappers, M. Wei, M. G. Blamire and J. L. MacManus-Driscoll, *Adv. Mater.*, 2006, **18**, 1449.
- <sup>32</sup> J. M. D. Coey, M. Venkatesan and C. B. Fitzgerald, *Nat. Mater.*, 2005, **4**, 173.
- <sup>33</sup> D. Loss and D. P. DiVincenzo, *Phys. Rev. A*, 1998, **57**, 120.
- <sup>34</sup> C. Song, K. Geng, F. Zeng, X. Wang, Y. Shen, F. Pan, Y. Xie, T. Liu, H. Zhou and Z. Fan, *Phys. Rev. B*, 2006, **73**, 024405.
- <sup>35</sup> S. Ogale, R. Choudhary, J. Buban, S. Lofland, S. Shinde, S. Kale, V. Kulkarni, J. Higgins, C. Lanci, J. Simpson, N. Browning, S. Das Sarma, H. Drew, R. Greene and T. Venkatesan, *Phys. Rev. Lett.*, 2003, **91**, 077205.



**Figure and Table Captions**

**Fig. 1** (a)  $\theta$ - $2\theta$  XRD patterns, (b) enlarged view of  $\theta$ - $2\theta$  XRD patterns around  $38^\circ$ , (c) the Mn doping concentration dependence of  $(\bar{2}01)$  lattice plane distance, and (d) RHEED patterns of  $(\text{Ga}_{1-x}\text{Mn}_x)_2\text{O}_3$  thin films ( $x=0.06, 0.31$ ).

**Fig. 2** Mn and Ga SIMS depth profiles for  $(\text{Ga}_{0.47}\text{Mn}_{0.53})_2\text{O}_3$  thin film.

**Fig. 3** XPS spectra of Mn 2p and Ga 3d (inset) core level for  $(\text{Ga}_{0.47}\text{Mn}_{0.53})_2\text{O}_3$  thin film.

**Fig. 4** Absorption spectra of  $(\text{Ga}_{1-x}\text{Mn}_x)_2\text{O}_3$  ( $x=0.11, 0.31$ ) thin films compared with that of pure  $\beta\text{-Ga}_2\text{O}_3$  thin film and the plot of  $(ah\nu)^2$  versus  $h\nu$  in inset.

**Fig. 5**  $M$ - $H$  curves of  $(\text{Ga}_{1-x}\text{Mn}_x)_2\text{O}_3$  thin films at room temperature and temperature dependence magnetization of  $(\text{Ga}_{0.47}\text{Mn}_{0.53})_2\text{O}_3$  thin film at 2 kOe (inset).

**Table 1.** Magnetic parameters for  $(\text{Ga}_{1-x}\text{Mn}_x)_2\text{O}_3$  thin films with different Mn content.

The given  $M_s$  are at the magnetic field of 2 kOe.

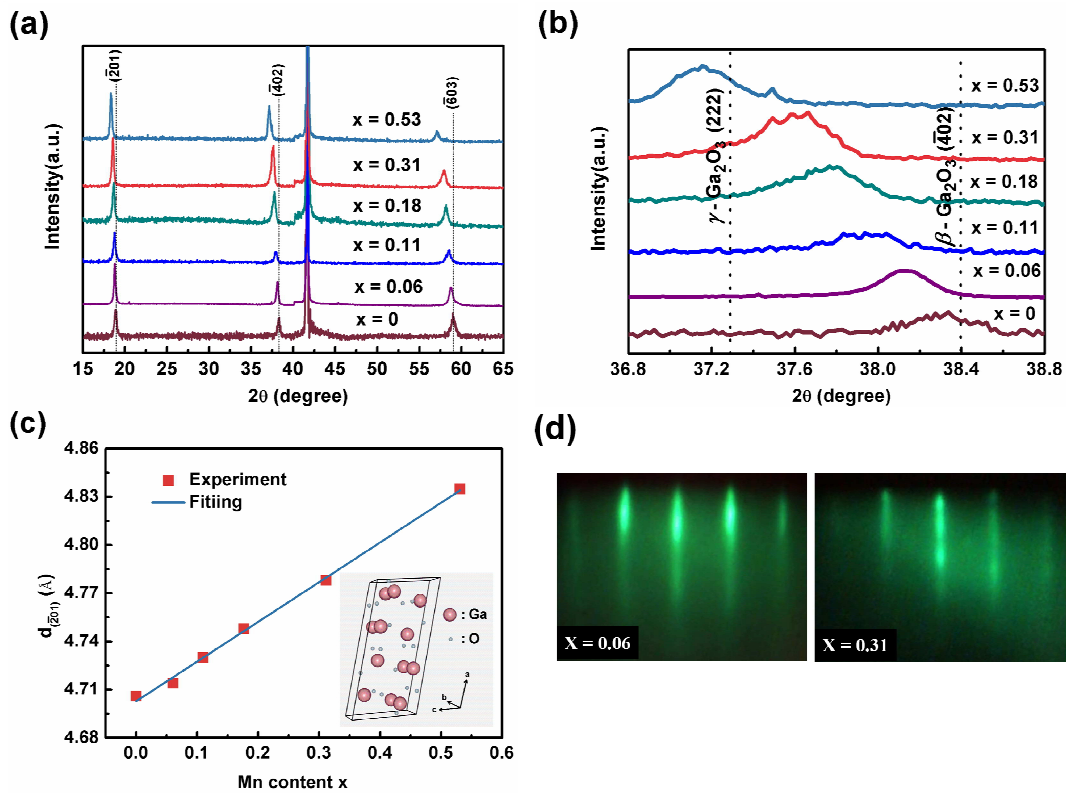


FIG. 1

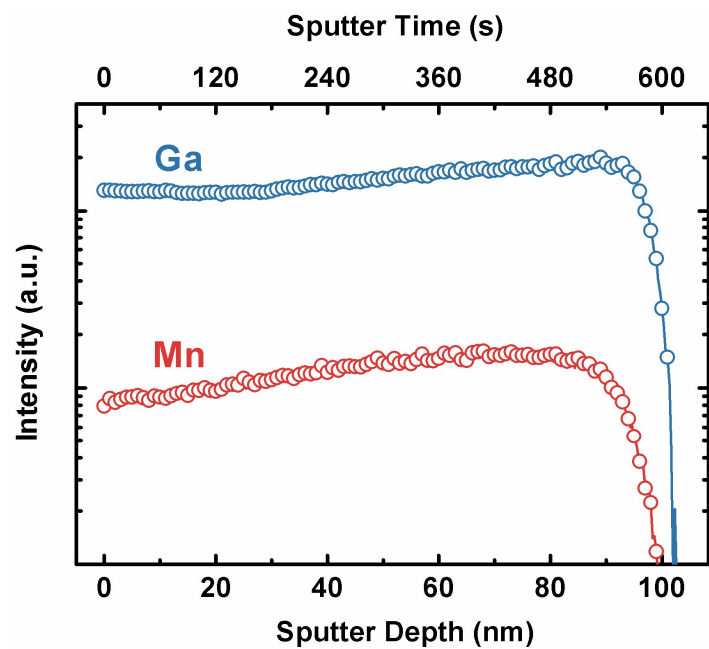


FIG. 2

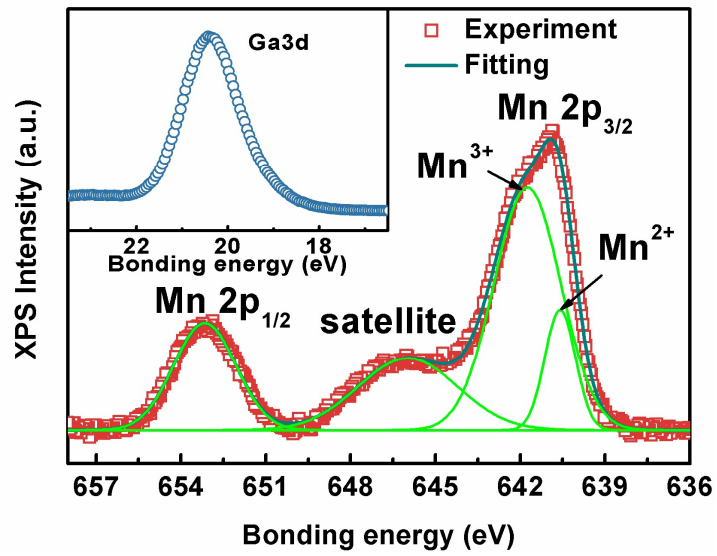


FIG. 3

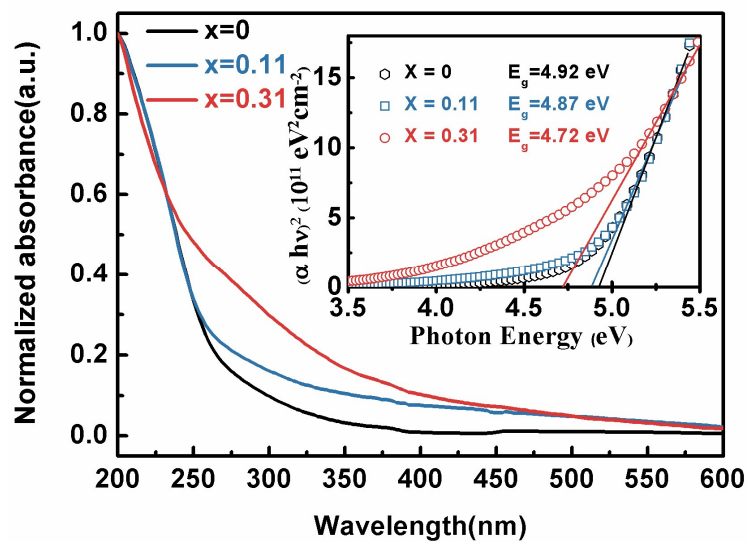


FIG. 4

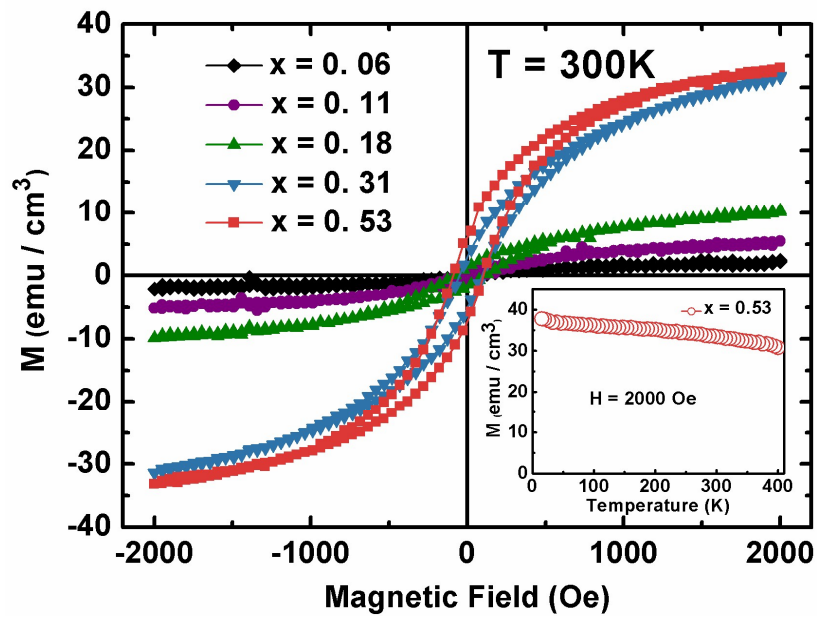


FIG. 5

Table 1

<b>Mn content (x)</b>	<b><math>M_s</math> (emu/cm<sup>3</sup>)</b>	<b>Coercivity (Oe)</b>	<b><math>M_r</math> (emu/cm<sup>3</sup>)</b>
<b>0.1097</b>	<b>5.5</b>	<b>62</b>	<b>0.8</b>
<b>0.1764</b>	<b>10.4</b>	<b>80</b>	<b>1.6</b>
<b>0.3117</b>	<b>31.6</b>	<b>98</b>	<b>5.4</b>
<b>0.5310</b>	<b>33.1</b>	<b>109</b>	<b>7.6</b>